



## OPEN ACCESS

## EDITED BY

Sabrina Lo Brutto,  
University of Palermo, Italy

## REVIEWED BY

Israel Anibal Vega,  
CONICET Dr. Mario H. Burgos Institute of  
Histology and Embryology (IHEM), Argentina  
Song Feng,  
Chinese Academy of Sciences (CAS), China

## \*CORRESPONDENCE

Liang Xiao

✉ xiaolian@smmu.edu.cn

Xueqi Ma

✉ mxqmmmm@163.com

Shuogui Xu

✉ shuogui\_xu@smmu.edu.cn

†These authors have contributed  
equally to this work and share  
first authorship

RECEIVED 19 January 2025

ACCEPTED 24 March 2025

PUBLISHED 15 April 2025

## CITATION

Liu X, Peng X, Wang J, Ju S, Sun Q, Ji W,  
Hua X, Zhang H, Höfer J, Pozzolini M,  
Xu S, Ma X and Xiao L (2025) Targeting  
metzincins to mitigate jellyfish blooms:  
a novel approach for conservation.  
*Front. Mar. Sci.* 12:1563258.  
doi: 10.3389/fmars.2025.1563258

## COPYRIGHT

© 2025 Liu, Peng, Wang, Ju, Sun, Ji, Hua,  
Zhang, Höfer, Pozzolini, Xu, Ma and Xiao. This  
is an open-access article distributed under the  
terms of the [Creative Commons Attribution  
License \(CC BY\)](https://creativecommons.org/licenses/by/4.0/). The use, distribution or  
reproduction in other forums is permitted,  
provided the original author(s) and the  
copyright owner(s) are credited and that the  
original publication in this journal is cited, in  
accordance with accepted academic  
practice. No use, distribution or reproduction  
is permitted which does not comply with  
these terms.

# Targeting metzincins to mitigate jellyfish blooms: a novel approach for conservation

Xuecun Liu<sup>1,2†</sup>, Xiao Peng<sup>1†</sup>, Jingqiang Wang<sup>3†</sup>, Shuhui Ju<sup>4</sup>,  
Qing Sun<sup>5</sup>, Wensai Ji<sup>6</sup>, Xiaoyu Hua<sup>1</sup>, Haiyan Zhang<sup>7</sup>,  
Juan Höfer<sup>8</sup>, Marina Pozzolini<sup>9</sup>, Shuogui Xu<sup>10\*</sup>, Xueqi Ma<sup>1\*</sup>  
and Liang Xiao<sup>1\*</sup>

<sup>1</sup>Department of Occupational and Environmental Health, Faculty of Naval Medicine, Naval Medical University (Second Military Medical University), Shanghai, China, <sup>2</sup>The Second Outpatient Department, NO.971 Hospital of the People's Liberation Army Navy, Qingdao, Shandong, China, <sup>3</sup>Department of Pharmacy, Shanghai Jiangong Hospital, Shanghai, China, <sup>4</sup>Thyroid and Breast Surgery, Changhai Hospital, Naval Medical University (Second Military Medical University), Shanghai, China, <sup>5</sup>Department of Military and Special Medicine, NO. 971 Hospital of the People's Liberation Army Navy, Qingdao, Shandong, China, <sup>6</sup>Medical Service Training Center, NO. 971 Hospital of the People's Liberation Army Navy, Qingdao, Shandong, China, <sup>7</sup>Department of Healthcare, Changhai Hospital, Naval Medical University (Second Military Medical University), Shanghai, China, <sup>8</sup>Escuela de Ciencias del Mar, Pontificia Universidad Católica de Valparaíso, Valparaíso, Región de Valparaíso, Chile, <sup>9</sup>Department of Earth, Environment and Life Sciences, University of Genova, Genova, Italy, <sup>10</sup>Department of Orthopedics, The First Affiliated Hospital of Naval Medical University: Changhai Hospital, Shanghai, China

**Introduction:** The modification of the marine ecological environment has led to the frequent occurrence of jellyfish blooms, causing global hazards. The budding reproduction of jellyfish polyps is a critical factor in their population size, yet there is limited understanding of the molecular mechanisms involved in this process. This study aims to explore the intrinsic regulatory factors of the budding of jellyfish *Aurelia coerulea* (*A. coerulea*) polyps from the perspective of jellyfish biotoxin and to develop new strategies for the management of jellyfish abundance.

**Methods:** The main biological toxins of the *A. coerulea* polyp were screened through the integrated analysis of transcriptomic and proteomic data. The broad-spectrum metalloproteinase inhibitor, ethylenediaminetetraacetic acid (EDTA), was employed to treat polyps for observing its effect on the budding of *A. coerulea* polyps. Through conducting the detection of metzincin proteolytic activity, molecular docking and kinetic analysis, as well as transcriptomic analysis and RT-qPCR verification before and after EDTA treatment of the polyp, the key biological toxins and the mechanisms influencing polyp budding were clarified.

**Results:** Four types of the metzincin family of metalloproteinases constituted the main biotoxins in the *A. coerulea* polyp. Among them, astacins (NAS) were the predominant metzincins of the *A. coerulea* polyp. We discovered that EDTA significantly inhibited the activity of metzincins and the budding of *A. coerulea* polyps. EDTA was capable of stably binding to the zinc-binding active sites of the

four major types of metzincins in the *A. coerulea* polyp and could down-regulate the expression levels of key metzincin molecules and enrich multiple pathways related to development.

**Conclusion:** This study elucidates the effects of metzincins on the budding of jellyfish polyps, providing a potential target for mitigating jellyfish blooms.

#### KEYWORDS

jellyfish bloom, *Aurelia coerulea* polyp, budding, metzincin, extracellular matrix

## 1 Introduction

Climate change, environmental pollution, and anthropogenic activities, such as eutrophication, overfishing, and the construction of nuclear power plants have led to alterations in the offshore ecological environment, thereby creating favorable conditions for the proliferation of jellyfish (Marques et al., 2019). In recent years, there has been a global proliferation of jellyfish, with at least 14 sea areas experiencing frequent blooms, including the Mediterranean Sea, the Gulf of Mexico, and the Sea of Japan. The scale and frequency of these blooms far exceed the capacity for self-regulation within marine ecosystems, leading to catastrophic consequences on a worldwide scale (Levy et al., 2024). Therefore, the prevention and control of jellyfish blooms in offshore waters is imminent for the marine ecological environment, human economic activities and human safety (Song et al., 2024). On the other hand, there exist tens of millions of cases involving jellyfish stings every year (Kan et al., 2016; Law, 2018; Mubarak et al., 2021; Edelist et al., 2023; Li et al., 2024a). Currently, the global management of jellyfish blooms primarily involves surveillance, early warning systems, interception measures, and salvage operations (Rowe et al., 2022; Gao et al., 2023; Song et al., 2024). However, the absence of dependable prevention and control measures for jellyfish blooms persists due to the high cost and inefficacy of conventional field surveillance and salvage operations (Bi et al., 2024; Levy et al., 2024). The underlying factors contributing to the surge in jellyfish populations may be another key point for prevention of jellyfish blooms.

As the main species of jellyfish blooms, scyphozoa exhibits a complex metagenic life cycle, encompassing sexual and asexual reproduction (Fuchs et al., 2014). The polyp stage primarily increases its population through asexual reproduction, either by budding for self-replication or by releasing strobilae via metamorphosis, and subsequently proceeds through the ephyrae stage, ultimately generating new jellyfish (Fuchs et al., 2014; Marques et al., 2019). The moon jellyfish *A. coerulea* is extensively distributed in coastal waters worldwide and serves as a well-established candidate for artificial breeding, within the class of scyphozoa jellyfish (Dong and Sun, 2018). It has been extensively

employed in research on asexual reproduction, including metamorphosis and budding (Gold et al., 2019; Khalturin et al., 2019; Weiland-Brauer et al., 2020). The majority of prior researches primarily focused on the influence of alterations in environmental factors on the occurrence of jellyfish blooms (Hubot et al., 2017; Dong and Sun, 2018). The deep insights into the polyp proliferation of *A. coerulea*, including the vital mechanisms and regulators in the process of proliferation, need to be further investigated. While there are some recent studies about the mechanism of metamorphosis in jellyfish polyps (Fuchs et al., 2014; Li et al., 2024b), the molecular mechanism of budding of jellyfish polyps remains inadequately understood.

The presence of biotoxins and their biotoxicity are fundamental biological traits exhibited by marine toxic jellyfish (Marchelek-Mysłiwiec et al., 2024; Yanagihara et al., 2024; Yasanga et al., 2025). It is crucial to emphasize that the biotoxins of jellyfish are not only in their nematocysts, but also extensively distributed throughout all of their tissues (Stabili et al., 2021). The transcriptome data of *Podocoryna*, *Clytia*, and *Aurelia* revealed significant differences in the expression levels of biotoxins in polyps compared to those in developing or adult medusae (Klompfen et al., 2021). Previous studies have confirmed that biotoxins show variations in different developmental stages in other animals, such as *Latrodectus tredecimguttatus* (Peng et al., 2020), or participate in the metamorphosis process, such as in the *Xenopus laevis* (Mathew et al., 2010). Hence, we hypothesize that the biotoxins in jellyfish, apart from exerting toxic effects (Kim et al., 2019), are highly likely to be related to life processes like development and proliferation. Studying the function of jellyfish biotoxins beyond their toxic effects is crucial for advancing our comprehension of the biological characteristics of jellyfish and their biotoxins.

In this study, we first identified metzincins as the prominent biotoxins of *A. coerulea* polyps, which was then confirmed to function in the process of asexual reproduction, characterized its three-dimensional structure and active binding sites, and explored the possible signaling pathway mechanism for budding. This study has significantly expanded our understanding on the life functions of jellyfish biotoxins, providing new insights into potential targets for controlling jellyfish populations in the changing marine environment.

## 2 Materials and methods

### 2.1 Animal and culture condition

Experimental animal *Aurelia coerulea* polyps, a species of the genus *Aurelia* (*Aurelia* sp.) (Ohdera et al., 2024), were cultured at the Naval Medical University in Shanghai, China. The feeding system for polyps was described in previous research (Wang et al., 2023). In brief, the polyps were fed with brine shrimp (*Artemia pathenogenetica*) every two days. Additionally, fresh artificial seawater was added two times per week, maintaining salinity levels between 28–32‰.

### 2.2 RNA extraction library construction and sequencing

Thirty polyps per sample were added to 400  $\mu$ L of SDS (Solarbio, China) mixture solution containing 10%  $\beta$ -mercaptoethanol (Sangon, China) in a tissue grinder for initial cracking. The specific RNA extraction method has been described in a previous research (Wang et al., 2023). The purity and concentration of RNA were measured using a Qubit 2.0 Fluorometer. The entire process of RNA extraction was carried out at 4°C.

The total RNA quantity and purity were analyzed using the Bioanalyzer 2100 and RNA 6000 Nano LabChip Kit (Agilent, USA). High-quality RNA samples with the RIN > 7.0 were used to construct the sequencing library. Poly(A) RNA was purified using the magnetic beads method. Finally, 2 $\times$ 150 bp paired-end sequencing (PE150) was conducted using the Illumina Novaseq<sup>TM</sup> 6000 platform (LC-Bio Technology, China). Subsequently, adapter contamination and low-quality reads were removed through the application of internal Cutadapt and Perl scripts following sequencing.

### 2.3 Total protein extraction and treatment

The proteins of *A. coerulea* polyps were extracted using the Protein Extraction Kit (Bangfei, China). The quantification of the proteins was performed using the Bradford method (Bradford, 1976). The protein samples were then reduced and alkylated with DTT and iodoacetamide (IAA) before being digested with trypsin using the FASP method.

### 2.4 HPLC and mass spectrometry analysis

Each sample was separated by a High-Performance Liquid Chromatography (HPLC) system and analyzed with the Orbitrap Fusion mass spectrometer (Thermo Scientific). The raw data in the RAW file was generated using Proteome Discoverer software (Thermo Scientific), with the *de novo* transcriptome used as a reference. The search parameters were set as follows: enzyme = trypsin, max missed cleavages = 2, fixed modifications = carbamidomethyl (C), variable modifications = oxidation (M),

acetyl (Protein N-term), peptide mass tolerance =  $\pm 7$  ppm, fragment mass tolerance = 20 mmu, peptide confidence = high.

### 2.5 Bioinformation analysis

All identified proteins were annotated in five authoritative databases, including the Gene Ontology (GO) (<http://www.geneontology.org>), Kyoto Encyclopedia of Genes and Genomes (KEGG) (<http://www.genome.jp/kegg/>), non-redundant (NR) protein database (<http://www.ncbi.nlm.nih.gov/>), SwissProt (<http://www.expasy.ch/sprot/>), and UniProt Knowledgebase (UniProtKB) (<https://www.uniprot.org/>) with a threshold of E-value < 0.00001. Multisequence alignment analysis was performed using BioEdit (Version: 7.0.5.3) under default parameters. The local BLAST tool was used with SwissProt and UniProtKB for screening toxins, employing a threshold E-value of less than  $10^{-5}$  to yield toxin-related genes at the transcriptome and proteome levels.

### 2.6 The construction of the budding model of *A. coerulea* polyps

New polyps were inoculated in 150 mm cell culture dish one week prior to the experiment to ensure their overall health. Before the experiment, select polyps without buds and with good tentacle extension for vaccination into the new single-well plate. Three polyps were set in each well as a biological replicate, and each group had four biological replicates ( $n = 4$ ). The four experimental groups were fed according to feeding cycles of two days (FM-per2), four days (FM-per4), seven days (FM-per7), and fourteen days (FM-per14), respectively. All the experimental units (the single-well plates with 3 polyps) were placed on the same layer of the 20°C incubator, and the experimental units were assigned to different treatment groups by using the simple randomization method. If a highly isolated layout occurred, the layout would be discarded, and then the randomization operation would be repeated until a layout with an acceptable degree of interleaving was obtained. The number of the polyp buds was observed and recorded every 24 hours for 14 days. The software GraphPad Prism 8.4.2 was used to create line graphs showing the number of the polyp buds in each group.

### 2.7 Treatments with metalloproteinase inhibitors on budding polyps

The metalloproteinase inhibitor EDTA (Bio-Light, China) is a broad-spectrum inhibitor of metalloproteinases (Li et al., 2019). ARP-100 (TargetMol, USA) is an effective and selective inhibitor of metalloproteinase MMP-2. The solid reagent was dissolved in ddH<sub>2</sub>O to a concentration of 1 mM and then further diluted with sterile seawater for the experiment.

The experimental group was treated with EDTA at the concentration of 600 nM, while the polyps in control group were kept in artificial seawater. The polyp budding observation experiment

was conducted according to Method 2.6. Three polyps were set in each well as a biological replicate, and each group had four biological replicates ( $n = 4$ ). The feeding cycle of FM-per4 (once every four days) was selected, and the observation period was seven days.

## 2.8 Metzincin proteolytic activity determination

Thirty polyps were collected and ultrasonically fragmented in each sample to create a homogenized mixture. RIPA lysate (Epizyme, China) and a protein phosphatase inhibitor (Solarbio, China) were added to each sample, followed by centrifugation at 10,000 g for 15 minutes. The supernatant subsequently collected was assessed using the BCA assay (Beyotime). According to the results of the BCA assay, each sample protein from both the experimental group and the control group was diluted to the same concentration before the activity of metzincins was detected.

Each sample was added to a solution of Azocasein (Sigma, USA) at pH 8.8 and incubated in a water bath at 37 °C for 90 minutes. Subsequently, 200  $\mu$ L of 0.5 M trichloroacetic acid (TCA) (Ronoen, China) was added to each sample and allowed to stand at room temperature for 30 minutes. The samples were then centrifuged at 10,000 g for 10 minutes, after which 100  $\mu$ L of the supernatant was collected from each sample and mixed with an equal volume of 0.5 M NaOH (Amresco, USA). The absorbance was subsequently measured at a wavelength of 450 nm. The protein extracted from 30 polyps was taken as one biological sample, and there were four biological replicates in each group.

## 2.9 Transcriptome analysis of EDTA-treated polyps

Both the experimental group and the control group had four replications, with 36 polyps in each group. According to 2.7, the polyps in the experimental group were treated with 600 nM EDTA seawater, while those in the control group were treated with sterile seawater. Total RNA was extracted after four days of treatment and the RNA libraries were sequenced on the illumina Novaseq<sup>TM</sup> 6000 platform by LC Bio Technology CO., Ltd (Hangzhou, China).

## 2.10 RT-qPCR

Following the isolation of total RNA, mRNA was transcribed into cDNA using a Bio-Rad PCR instrument and REverTra qPCR RT Master Mix (Toyobo, Japan) in accordance with the manufacturer's protocol. The primers for amplifying these genes (Supplementary Table S1) were synthesized by Sangon Biotech (Shanghai, China). Each amplification system contained SYBR Green qPCR Master Mix (TargetMol, USA), primers, target gene cDNA, and DEPC water added to make a total volume of 20  $\mu$ L. The reactions were carried out using an Eppendorf MasterCycler realplex2 with an initial denaturation at 95°C for 5 minutes, followed by 40 cycles of 94°C for 10 seconds, 60°C for 20 seconds, and 72°C for 30 seconds. A final extension was performed at 72°C for 5 minutes. The terminations of

SYBR Green I density and cycle threshold (Ct) values were analyzed using CFX management software (Bio-Rad, USA). The gene expression levels were estimated using the best comparative Ct value ( $2^{-\Delta\Delta Ct}$ ) method.

## 2.11 Evolutional analysis

The coding sequences of four types of metzincins were organized into a fasta file. The MUSCLE method was used for sequence alignment, and then the phylogenetic tree was analyzed by Maximum Parsimony (MP) in MEGA7 software. The most parsimonious tree with length = 3077 is shown. The consistency index is 0.182970 (0.182439), the retention index is 0.271304 (0.271304), and the composite index is 0.049641 (0.049497) for all sites and parsimony-informative sites (in parentheses). The MP tree was obtained using the Subtree-Pruning-Regrafting (SPR) algorithm with search level 0 in which the initial trees were obtained by the random addition of sequences (10 replicates). The analysis involved 48 nucleotide sequences. Codon positions included were 1st+2nd+3rd+Noncoding. All positions with less than 95% site coverage were eliminated.

## 2.12 Molecular docking and dynamic simulation

The receptor peptides were found and extracted from the *A. coerulea* polyps. The structure of all peptides was predicted using AlphaFold2 (Bryant et al., 2022), and the PDB file was selected as the predicted file for the receptor. The 3D SDF format file (Compound CID: 6049) of small molecule ligand EDTA can be downloaded from the website <https://pubchem.ncbi.nlm.nih.gov/>. Pre-processing and docking of all receptors and ligands were performed using AutoDock Vina software (Eberhardt et al., 2021). First, all files of the receptor and ligand are transformed into PDBQT files, then the docking sites of the receptor protein are predicted to screen out the best conformation for binding to the ligand. After docking with a small molecule ligand, analysis was performed on the website <https://plip-tool.biotech.tu-dresden.de/plip-web/plip/index> to identify non-covalent interactions between protein and small molecule ligands. Finally, the representative molecules were selected to be combined with EDTA for molecular dynamics simulation.

## 2.13 Statistical analysis

All data were expressed as mean  $\pm$  standard deviation (SD). The Shapiro-Wilk method was used to test whether the two variables of the control group and the experimental group in RT-qPCR followed a normal distribution, and then analysis of variance was performed. For data that did not follow a normal distribution, the rank sum test was used. For data that followed a normal distribution and had homogeneous variance, the independent sample t-test was used; for

data with heterogeneous variance, the Welch-corrected t-test was used to analyze the data. Statistical significance was set at \* $P < 0.05$ , \*\* $P < 0.01$ , \*\*\* $P < 0.001$ , and \*\*\*\* $P < 0.0001$ . Statistical analysis was conducted on the difference in metzincin proteolytic activity of polyps before and after metalloproteinase inhibitor treatment by employing the same method as that of RT-qPCR. The column charts were drawn by GraphPad Prism 8.4.2.

## 3 Results

### 3.1 Metzincins were identified as the key biotoxin components of jellyfish polyps

In order to explore the potential role of biotoxins in regulating the growth and development of jellyfish, we conducted transcriptomic and proteomic analyses on jellyfish *A. coerulea* polyps (Figures 1A, B, Supplementary Figures S1, S2). Subsequently, the data from our combined transcriptome-proteome analysis were carefully screened to identify unigenes potentially associated with biotoxins and biotoxin proteins (Figure 1C), including major biotoxin families such as metalloproteinases, latrotoxin, and calglandulin. In the polyp of *A. coerulea*, the expression of metalloproteinases topped the list at the transcriptional level and was among the top three at the protein level (Figures 1D, E). Notably, metalloproteinases were the most abundant in quantity at both transcriptional (Figure 1D) and protein levels (Figure 1E). Specifically, we identified a total of 50 metalloproteinases at the transcriptome level and 17 at the proteome level, collectively representing 32% and 24% of the top eight biotoxins in transcriptions and proteome, respectively.

Our data showed that metalloproteinases in the *A. coerulea* polyps predominantly existed in four forms: NAS, matrix metalloproteinases (MMPs), a disintegrin and metalloproteinases (ADAMs) and a disintegrin and metalloproteinase with thrombospondin motifs (ADAMTSs). All these members belong to the metzincin superfamily of the metalloproteinases (Rivera et al., 2010). Despite their presence in different subtypes, the evolutionary relationship between metzincins was observed to be closely related (Figure 1J). Moreover, among the four metzincins, the quantity and overall expression of NAS were the highest (Figures 1F–I). Four unigenes that were relatively highly expressed in the transcriptome (Figure 1F) were selected for RT-qPCR verification, which confirmed the reliability of the data (Supplementary Figure S3). Overall, the integrated analysis of transcriptome-proteome data reveals that metzincins are the key biotoxin components in *A. coerulea* polyps.

### 3.2 EDTA suppresses the activity of metzincins and inhibits the budding of jellyfish polyps

Figure 2A illustrates the complete process of the budding of *A. coerulea* polyps and subsequent detachment from the parental organism in the model. Based on the observed variations in polyp

budding rates at different feeding frequencies, we developed a model of the budding of *A. coerulea* polyps, revealing a positive correlation between increased feeding frequency and enhanced budding (Figure 2B). To optimize experimental efficiency and efficacy, we determined that feeding every four days would be the subsequent experimental condition. To investigate the impact of inhibiting metzincins on the budding of *A. coerulea* polyps, a broad-spectrum metalloproteinase inhibitor, EDTA, was employed to treat the polyps. During the experimental observation period (seven days), the number of the polyp buds in the EDTA-treated group was consistently lower than that in the control group (Figure 2C, Supplementary Figure S4A), indicating a restraint in budding.

Furthermore, the assessment of metzincin activity demonstrated that the total protein of polyps exhibited strong metzincin activity, which showed a positive correlation with the concentrations of the protein of polyps (Figure 2D). Following EDTA treatment of the polyps, there was a decrease in metzincin activity in the total protein of polyps (Figure 2E, Supplementary Figure S4B). These findings suggest that EDTA negatively regulates the process of the budding of *A. coerulea* polyps, potentially by inhibiting metzincin activity.

### 3.3 EDTA inhibited the activity of metzincins through binding to their zinc binding active site

We selected 26 representative metzincin molecules from the transcriptome of *A. coerulea* polyps to elucidate the mechanism of interaction between EDTA and four types of metzincins. AlphaFold2 was used to predict the 3D spatial structure of the molecular proteins mentioned above, and then they were docked with EDTA. The binding energy values are displayed in Figure 3A. Among the four metzincins, the receptor polypeptides that exhibited the closest binding affinity to EDTA, or is most representative, are as follows: ADAM: CTG-72.172 (-6 kJ/mol), ADAMTS: CTG-109.158 (5.3 kJ/mol), MMP: CTG-132.73 (5.7 kJ/mol), and NAS: CTG-120.86 (-6 kJ/mol) and NAS: CTG-27.246 (-4.4 kJ/mol) (Figure 3A, Supplementary Tables S2, S3). Further docking analysis and kinetic simulation were conducted for these five receptor polypeptides. Through non-covalent interaction analysis, it was observed that these five metzincins are capable of binding to EDTA and forming hydrogen bonds and salt bridges. The bindings of the five metzincins receptor polypeptide with EDTA were all located in the central region of the receptor space, surrounded by elongated protein helices (Figures 3B–F).

In the aforementioned molecular docking, NAS and ADAM receptor polypeptides are the most susceptible to bind with EDTA. Moreover, both NAS receptor polypeptides, namely CTG-120.86 and CTG-27.246, can spontaneously bind to EDTA. Hence, we focused on these two NAS metzincins for the further exploration of the mechanism by which EDTA inhibits metzincin activity. CTG-120.86 and CTG-27.246 are NAS with similar structures, characterized by Pre-Pro-Sequences, astacin domain, epidermal growth factor-like modules, CUB domain, and Thrombospondin type 1 domains (TSP1) (Figure 3G). The CTG-120.86 astacin domain contains a

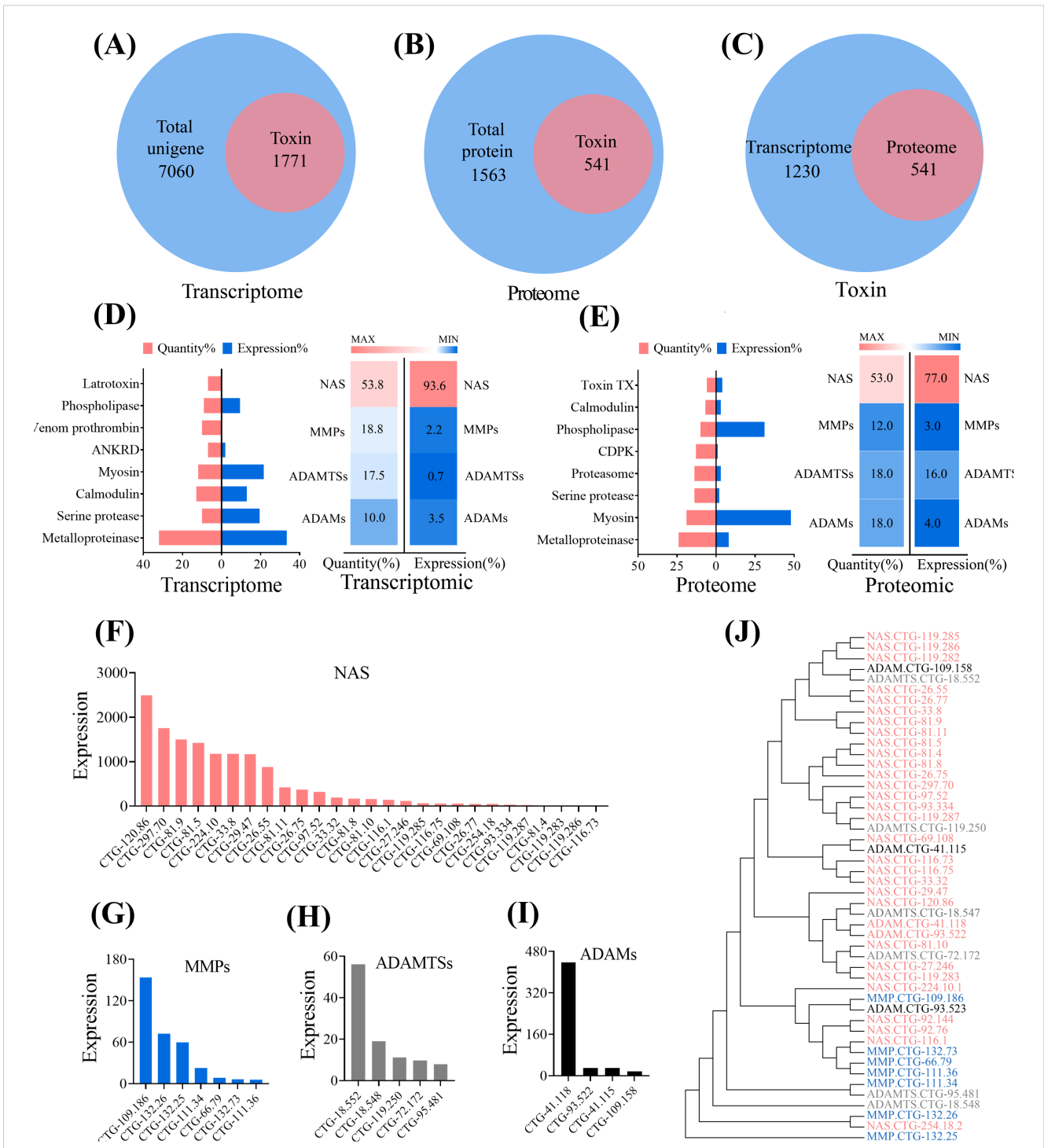


FIGURE 1

The analysis of toxic components of *A. coerulea* polyps. (A) Venn diagram analysis of the toxin unigenes with the total unigenes in the *A. coerulea* polyp transcriptome. (B) Venn diagram analysis of the toxin proteins with the total proteins in the *A. coerulea* polyp transcriptome. (C) Venn diagram analysis of toxins in the proteome and the transcriptome of *A. coerulea* polyps. (D) Right: The *A. coerulea* polyp transcriptome encompasses eight major toxin families, including Metalloproteinase, Calglandulin, Serine protease, Venom prothrombin, Latrotoxin, Thrombin, Coagulation factor and Phospholipase; Left: The composition of metalloproteinases in the *A. coerulea* polyp transcriptome. (E) Right: The *A. coerulea* polyps proteome contains eight major toxin families, including Metalloproteinase, Myosin, Serine protease, Proteasome, CDPK, Phospholipase, Calmodulin and Toxin TX; Left: The composition of metalloproteinases in the *A. coerulea* polyp proteome. (F) The expression of astacins (NAS) in the *A. coerulea* polyp transcriptome. (G) The expression of matrix metalloproteinases (MMPs) in the *A. coerulea* polyp transcriptome. (H) The expression of a disintegrin and metalloproteinase with thrombospondin motifs (ADAMTSs) in the *A. coerulea* transcriptome. (I) The expression of a disintegrin and metalloproteinases (ADAMs) in the *A. coerulea* transcriptome. The (F–I) expression values were calculated based on the FPKM values of the corresponding genes. (J) An evolutionary tree analysis of metalloproteinases of the *A. coerulea* polyps. The evolutionary history was inferred using the Maximum Parsimony method.

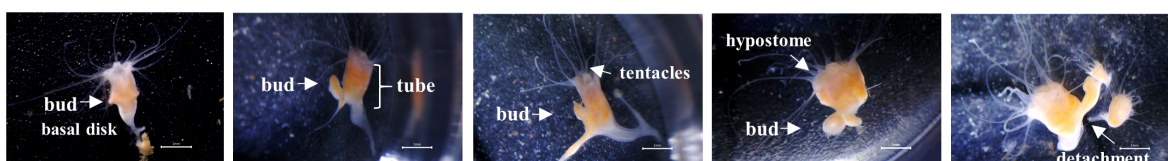
very specific base sequence HEXXHXGXFXHEXXRXDRD (HEIMHAIGFYHEQSRRDRD), also known as the zinc active site. CTG-120.86 is composed of 11  $\alpha$ -helices and eight  $\beta$ -sheets, and CTG-27.246 is composed of 10  $\alpha$ -helices and 14  $\beta$ -sheets, with the zinc-binding active site located in the middle of the polypeptide (Figure 3H). Although the binding region remains consistent, there were differences in the residues involved in protein interactions. EDTA can form hydrogen bonds with GLU159, ASN216, and GLN227 on CTG-120.86 protein. Additionally, it was observed to form salt bridges with HIS148, HIS152 and ASP224. In contrast, in CTG-27.246 protein, EDTA formed salt bridges with ARG176 and simultaneously formed hydrogen bonds with GLN175, GLY179, TYR249, GLN251, and TYR253. The stability of the CTG-120.86 and CTG-27.246 bound to the EDTA conformation was verified through molecular dynamics (MD) simulations, which showed that the SASA values of both docking complexes gradually decreased and subsequently stabilized over time (Figures 3I, J). The RMSD value of the CTG-27.246 docking complex simulation was more stable than that of CTG-120.86. In CTG-27.246, the RMSD value gradually increased and tended to stabilize, while 120.86 showed a constant fluctuation trend (Figures 3K, L).

Therefore, we speculated that EDTA was able to bind stably to metzincins such as NAS and most likely inhibited the activity of metzincins by preventing zinc ions from binding to their Zn-binding active sites.

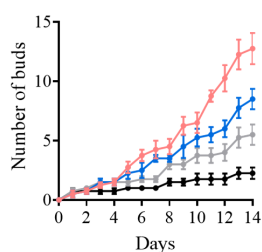
### 3.4 EDTA treatment of polyyps downregulated the expression of metzincins

Through RNA sequencing analysis of the polyyps treated with EDTA, we further explore the alterations in the gene expression of metzincins in *A. coerulea* polyyps and acquire an understanding of the molecular mechanisms underlying the negative regulation of the budding of the polyyps treated with EDTA. A total of 10,752 genes were sequenced, and 285 expressed biotoxin genes were obtained through local BLAST analysis of transcriptome genes and databases. The biotoxin categories were ranked in accordance with the number of genes, among which metzincins held the top position, followed by serine protease and phospholipase (Supplementary Figure S5). There were 34 metzincin genes, consisting of NAS, MMPs, ADAMTs and ADAMs, and NAS were found to be the most abundant, accounting for 55.8% of the total number of metzincin genes (Figures 4A–D). Compared to the control group, the expression of CTG-27.246 (NAS-4) was significantly down-regulated in the EDTA-treated group, and there was a downward trend in the expression of 19 metzincin genes (Figure 4E). The top four down-regulated metzincin genes were chosen for RT-qPCR validation. The results of the RT-qPCR analysis confirmed that the alterations in the expression levels of these genes were in accordance with the sequencing findings. Specifically, NAS-4 (CTG-27.246),

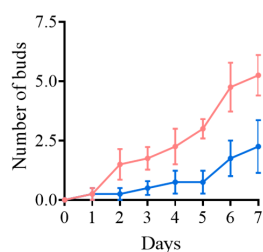
(A)



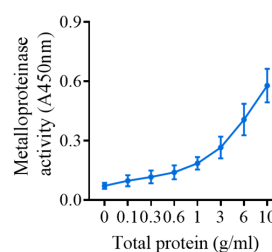
(B)



(C)



(D)



(E)

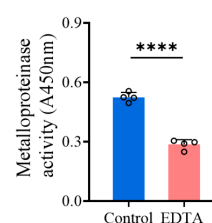
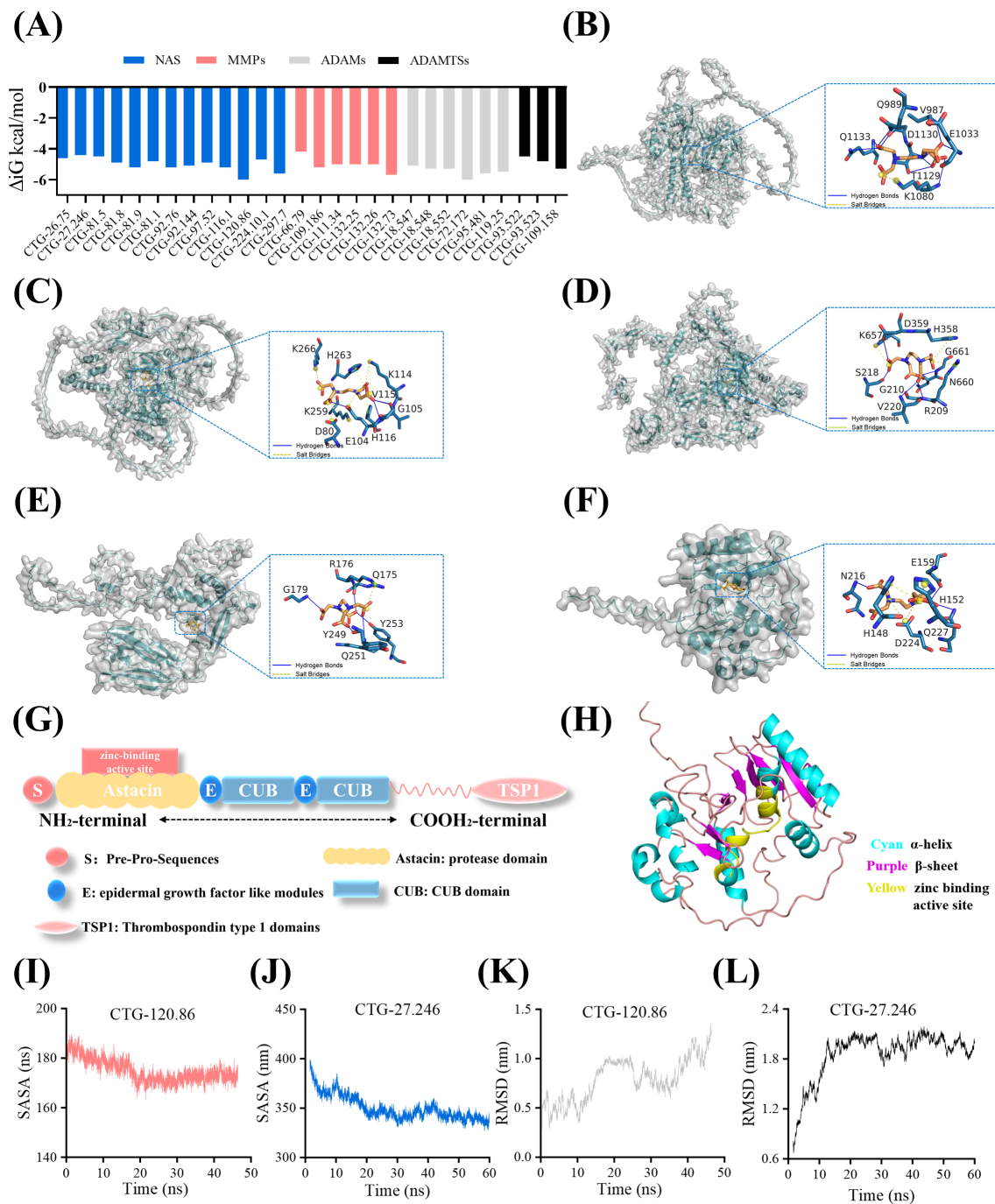


FIGURE 2

The polyp budding is inhibited by EDTA. (A) The process of budding in *A. coerulea* polyyps. Scale bar: 1 mm. (B) Construction of a budding model for the polyyps of *A. coerulea*; Feeding Model FM-per2, FM-per4, FM-per7 and FM-per14 represent feeding every two, four, seven, and fourteen days respectively. Three polyyps were set in each well as a biological replicate, and each group had four biological replicates ( $n = 4$ ). (C) Effects of EDTA treatment on the budding of *A. coerulea* polyyps. The feeding model FM-per4 was used and the experiment lasted for seven days. Three polyyps were set in each well as a biological replicate, and each group had four biological replicates ( $n = 4$ ). (D) Metzincin activity of total polyp protein at different concentrations. (E) Metzincin activity of the polyyps before and after treated with EDTA. (D, E) The protein extracted from 30 polyyps was taken as one biological sample, and there were four biological replicates in each group. Data are presented as mean  $\pm$  SD ( $n=4$ ). \*\*\*\* $P < 0.0001$ .



**FIGURE 3**  
 EDTA inhibits the activity of metzincins through binding to their zinc binding active site. **(A)** The docking binding energy values of 26 representative metzincin receptor proteins and the ligand EDTA. The screening criteria for the 26 representative metzincin molecules were that each molecule had an FPKM value greater than six and an expression level within the top 34% of its category. **(B)** Schematic diagram of molecular docking between CTG-132.73 and EDTA. **(C)** Schematic diagram of molecular docking between CTG-109.58 and EDTA. **(D)** Schematic diagram of molecular docking between CTG-72.172 and EDTA. **(E)** Schematic diagram of molecular docking between CTG-27.246 and EDTA. **(F)** Schematic diagram of molecular docking between CTG-120.86 and EDTA. The dotted box in B-F indicates the molecular docking site. **(G)** Schematic representation of the NAS structure. **(H)** 3D structure simulation of CTG-120.86 protein. **(I, J)** SASA fluctuation curves of CTG-120.86 **(I)** and CTG-27.246 **(J)** docking with EDTA. **(K, L)** RMSD fluctuation curves of CTG-120.86 **(K)** and CTG-27.246 **(L)** docking with EDTA.

ADAMT-6 (CTG-18.548), NAS-4 (CTG-116.73) and MMP-25 (CTG-132.73) exhibited significant down-regulation in EDTA-treated polyps ( $P < 0.05$ ) (Figures 4F–I). The results indicated that EDTA treatment could attenuate the expression of key metzincin molecules in polyps.

Based on the criteria of  $|\log_2FC| \geq 1$  and  $P < 0.05$ , a substantial number of differentially expressed genes were identified between the EDTA-treated group and the control group, comprising 126 up-regulated genes and 42 down-regulated genes (Figure 4J). GO enrichment analysis was conducted on these differentially

expressed genes and disclosed the 15 most significant GO terms, which pertained to three GO categories. Among them, the transporter activity was the sole one belonging to Molecular Function. The most enriched genes in the Cellular Component were membrane and cytoplasm, signifying the location of the gene product within the cell. The canonical Wnt signaling pathway and cell differentiation were the most enriched genes in Biological Process, mirroring the relevance to biological development (Figure 4K). KEGG analysis indicated that out of the Top 15

pathways exhibiting significant differences before and after EDTA treatment of polyps ( $P < 0.05$ ), eight were linked to growth and development (Figure 4L). Among these pathways, the Notch signaling pathway displayed the most notable distinction, followed by ECM-receptor interaction. The GSEA analysis of the Notch pathway disclosed that the enrichment score (ES) amounted to 0.5018, and the significant p-value was 0.0056 ( $< 0.05$ ). Concurrently, the differentially expressed genes enriched in the Notch pathway were conspicuously upregulated (Figure 4M). These

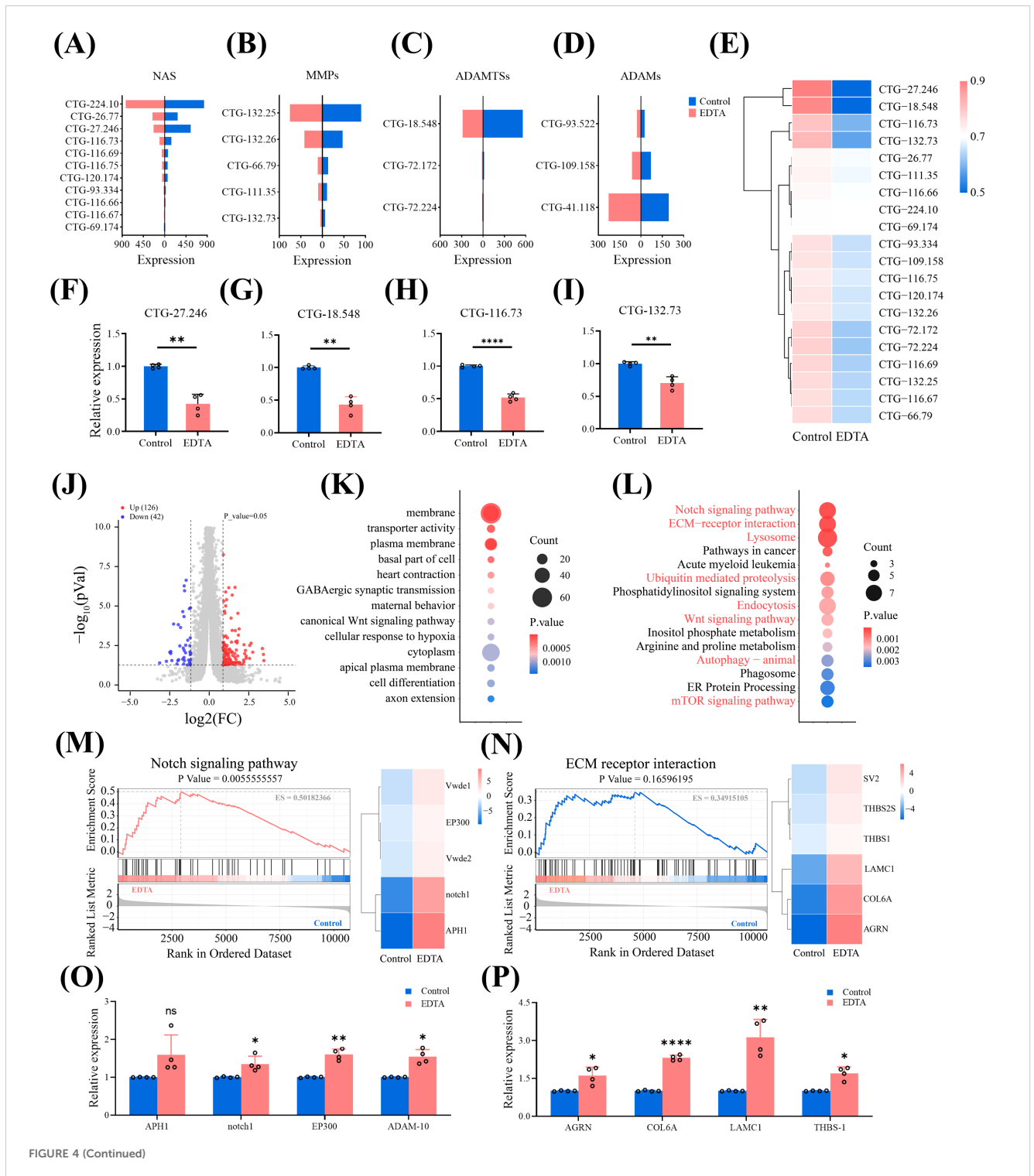


FIGURE 4 (Continued)

## FIGURE 4 (Continued)

Transcriptomic analysis of polyps treated with EDTA (A–E). The expression of NAS (A), MMPs (B), ADAMTSs (C) and ADAMs (D) was compared between the control group and the EDTA-treated group. The gene expression of the EDTA treated group is indicated in red, while that of the control group is indicated in blue. (E) Heat map showing the expression of 20 metzincins that were downregulated in the *A. coerulea* polyp treated with EDTA. (F–I) RT-qPCR results of the expressions of CTG-27.246 (F), CTG-18.548 (G), CTG-116.73 (H) and CTG-132.73 (I) before and after EDTA treatment. RNA was extracted from 20 polyps as one biological sample, and there were four biological replicates in each group. Data are presented as mean  $\pm$  SD (n=4). \*P < 0.05, \*\*P < 0.01, and \*\*\*P < 0.001. (J) A volcano plot of the differentially expressed screened in the control and EDTA treated groups, in which the red indicates the differentially upregulated genes and the blue indicates the differentially downregulated genes. (K) Top 15 differentially enriched GO pathways. (L) Top 15 differentially enriched KEGG pathways. The pathways highlighted in red denote pathways that are developmentally significant. In Figure (K, L), the size of the bubble shows the number of matched unigenes in the pathway, and the color represents the P value. (M) Left: Differential expression GSEA plot of the Notch pathway in polyps. Right: Heatmap of differentially expressed signaling molecules enriched in the Notch pathway. (N) Left: Differential expression GSEA plot of the ECM-receptor interaction pathway in polyps. Right: Heatmap of differential gene expression on the ECM-receptor interaction pathway in polyps. (O) RT-qPCR results of the expressions of the representative upregulated genes enriched in the notch pathway and ADAM-10 before and after EDTA treatment. (P) RT-qPCR results of the expressions of the ECM-receptor interaction pathway before and after EDTA treatment. (O, P) RNA was extracted from 20 polyps as one biological sample, and there were four biological replicates in each group. Data are presented as mean  $\pm$  SD (n=4). \*P < 0.05, \*\*P < 0.01, \*\*\*P < 0.001 and \*\*\*\*P < 0.0001.

outcomes signified that the Notch pathway was significantly upregulated in polyps subsequent to EDTA treatment. The GSEA analysis of the ECM-receptor interaction pathway revealed that the enrichment score (ES) was 0.3496 and the p-value was 0.1660 (> 0.05), suggesting that the ECM-receptor interaction pathway merely exhibited an upward tendency following EDTA treatment, yet was not statistically significant. Nevertheless, it is notable that the ECM-related genes enriched in the ECM-receptor interaction pathway were significantly upregulated (Figure 4N). We respectively screened the representative upregulated genes enriched in the Notch pathway and the ECM-receptor interaction pathway, as well as a related upregulated metzincin gene, ADAM10, and performed RT-qPCR verification. It was found that the expression changes of these genes were consistent with the RNA-seq expression profile (Figures 4O, P).

The data indicated that EDTA treatment down-regulated the expression of metzincins and enriched a number of developmental pathways and biological processes.

## 4 Discussion

This study reveals the important role and potential regulatory mechanism of metzincins in the budding of jellyfish polyps. Through combined omics analysis, we have identified the key metzincin NAS in *A. coerulea* polyps. The inhibition of polyp budding was observed following EDTA treatment. Further validation through metzincin activity assay, molecular dynamics analysis, and transcriptome analysis has confirmed that EDTA inhibits the activity of metzincins and alters expression levels.

The presence of biotoxins in marine jellyfish is highly abundant. Previous researches have indicated variations in the expression levels of biotoxins across different growth and development stages of jellyfish (Klompfen et al., 2021; Li et al., 2022). This study specifically investigated the biotoxin gene and protein expression of *A. coerulea* polyps, revealing that metzincins hold a prominent position among them. Our data revealed the presence of four prominent classes of the metzincin family of metalloproteinases in *A. coerulea* polyps, namely NAS, MMPs, ADAMTSs and ADAMs (Rose et al., 2021). Metzincins play a crucial role in

various biological growth and development processes, including mammalian gonadal development (Livermore et al., 2019; Li et al., 2023), animal bone regeneration (Keow et al., 2011), sea urchin hatching (Morgulis et al., 2021; Chiarelli et al., 2025), and intestinal regeneration in sea cucumber (*Apostichopus japonicus*) (Miao et al., 2017). The metzincin superfamily is composed of Zinc-metalloproteinases that play a crucial role in remodeling the ECM by degrading ECM components (Apte and Parks, 2015), activating cell surface proteins, and shedding membrane-bound receptor molecules. However, the function of these metzincins in jellyfish remains unknown. Through combined transcriptomic and proteomic analysis, we identified NAS as the predominant metzincins in *A. coerulea* polyps, and they are likely to exert a crucial role in the growth and development of jellyfish polyps by decomposing and remodelling the ECM (Sterchi et al., 2008; Becker-Pauly et al., 2011). Furthermore, among the genes enriched in the transcriptome in which the budding of polyps was inhibited following EDTA treatment, metzincins still consisted of NAS, MMPs, ADAMTs, and ADAMs, with NAS ranking first. This further substantiates the dominant position of NAS in polyps and its potential role in development.

It has been demonstrated that the extended N-terminal propeptide plays a role in conferring a latent period to NAS in eukaryotes, resulting in the secretion of most NAS as inactive zymogens. After combining with zinc ions, the molecular conformation of NAS changes, leading to the formation of the competent N-terminus (Gomis-Ruth et al., 2012). In this study, we performed 3D structural simulations of metzincins represented by NAS and identified the central location of the polypeptide as the active site for zinc binding, which is consistent with the findings of previous studies (Cerdà-Costa and Gomis-Rüth, 2014). Further molecular docking analysis of the broad-spectrum metalloproteinase inhibitor EDTA with metzincins peptides has revealed that the binding sites are also located within the central region of the ligand polypeptide space. Combined with the results of molecular dynamics, it can be inferred that EDTA could inhibit the activity of metzincins by stably binding to the zinc-binding active site of *A. coerulea* polyp metzincins, especially NAS. This differs from the previously widespread understanding that EDTA reduces the activity of metzincins by chelating the requisite divalent ions (Marino and Funk, 2012; García-López et al., 2023), and it constitutes a novel

supplement to EDTA for metalloproteinases. In the experiment on budding intervention in *A. coerulea* polyps, EDTA showed a significant adverse effect on the budding of *A. coerulea* polyps. Meanwhile, the metzincin activity of the total protein in EDTA-treated polyps exhibited a significant decrease compared to that of the control polyps. Taken collectively, EDTA significantly inhibited the activity of metzincins by stabilizing the zinc-binding active site of metzincins and directly chelating free zinc ions.

During budding, the body epithelial cells in the body column region of cnidarian polyps migrate along with the ECM and eventually give rise to new individuals (Aufschnaiter et al., 2011). In this process, epithelial cells undergo random movement on a mobile matrix, and the matrix moves in a directed manner towards the target location to form new buds (Matsubayashi, 2022). In contrast to the migration of epithelial cells, the ECM requires biochemical remodeling for shape alteration. During the early stage of budding, ECM disassembly and remodeling, rather than new ECM synthesis, are crucial for the budding of the polyps (Aufschnaiter et al., 2011). The metzincin family exerts a broad range of degradation effects on the ECM and constitutes an important enzyme family that regulates the dynamic equilibrium of ECM. For example, NAS can act on ECM proteins, such as laminin, collagen IV, and adhesion molecules, and influence morphogenesis by cutting and modifying the structural or mechanical properties of the ECM (Sarras et al., 2002; Apte and Parks, 2015), exerting pro-migratory effects on cells (Peters and Becker-Pauly, 2019). Whether it is the inhibition of the activity of metzincins or that of their transcription, it will exert a severe impact on ECM degradation. In this study, we confirmed that EDTA treatment reduced the activity of metzincins in *A. coerulea* polyps and downregulated the expression levels of key metzincins. Meanwhile, we observed evidence of restricted ECM degradation and excessive deposition. Transcriptome data showed that, compared with the control group, in the polyps treated with EDTA, laminin (LAMC1, CTG-95.548) and agrin (AGRN, CTG-91.129), both components of the basement membrane (BMs), were significantly upregulated. Additionally, collagen VI protein (COL6A, CTG - 84.172, CTG - 84.72) was also significantly upregulated. The decomposition and remodeling of the ECM are inhibited, leading to the decreased migratory ability of epithelial cells and the ECM in polyps, and then exerting a negative regulatory effect on the budding of polyps. This is consistent with the phenomenon in our research results, that is, treating polyps with EDTA will lead to a reduction in the number of new buds of polyps.

EDTA also regulates the expression level of metzincins in polyps through signal transduction, inhibits ECM decomposition, and affects the budding of *A. coerulea* polyps. In this study, multiple developmental related pathways were enriched in the transcriptome of the EDTA-treated polyps, among which the Notch pathway and the ECM receptor interaction pathway were the two most significantly different pathways. The thrombospondin-1 (THBS-1, CTG-131.382) and thrombospondin-2 (THBS-2, CTG-72.63) genes, which were enriched in the ECM-receptor interaction pathway, were significantly up-regulated. Among the differentially expressed genes

in the pathway, THBS-1 exhibited the highest fold change ( $\text{Log}_2\text{FC} = 12.24$ ). The up-regulated THBS-1 could further down-regulate the expression of metzincins and induce the up-regulation of the crucial ECM structural proteins COL6A, LAMC1, and AGRN, thereby impeding the disassembly and remodeling of ECM (Vadon-Le Goff et al., 2015; Chen et al., 2024). Intriguingly, contrary to previous reports suggesting that THBS-1 mainly regulates MMP (Chen et al., 2024), NAS-4 and ADAMT-6 also exhibited down-regulation in our validation results. However, our research in this aspect is limited, and whether the changes in the expression of metzincins other than MMP are caused by the changes in THBS-1 and whether they are directly regulated by THBS-1 need to be investigated through separate intervention of THBS-1 in *A. coerulea* polyps and additional molecular biology experiments.

Previous *in vitro* investigations regarding the activation of the Notch pathway by EDTA have disclosed that EDTA is capable of chelating extracellular free  $\text{Ca}^{2+}$  and undermining the binding stability of the two subunits of Notch heterodimers, resulting in the dissociation of the Notch extracellular domain and the release of its inhibition on the intrinsic active Notch intracellular subunit. This subsequently activates Notch receptors (Liu et al., 2024b). In the present study, we have made a further addition to the mechanism by which EDTA activates the Notch pathway. In the transcriptome data of EDTA-treated polyps, Notch-pathway-enriched molecules were significantly up-regulated. In addition, ADAM10 (CTG-41.118) showed a different up-regulation trend compared with other metzincins. These results indicate that EDTA activates the Notch receptor notch1 (CTG-221.43, CTG-224.18, CTG-231.59) by chelating extracellular free  $\text{Ca}^{2+}$ , followed by the combination of the Notch receptor with the ligand. The up-regulation of ADAM-10 caused by EDTA treatment promotes the processing of ADAM-mediated receptor-ligand complex (S2 cleavage) (Dornier et al., 2016; Defamie et al., 2024; Shimizu et al., 2024). Subsequently, the up-regulated  $\gamma$ -secretase (APH1, CTG- 64.98) complex mediates transmembrane cleavage (S3 cleavage), releasing the intracellular domain of Notch receptor (NECD) and facilitating its translocation to the nucleus. The acetyltransferase (EP300, CTG-95.191) is significantly up-regulated, leading to recruitment of acetylated histone (Kovall et al., 2017). This facilitates chromatin entry into the transcription complex, ultimately activating the Notch pathway and its effector molecules. Among these effector molecules, Myc-1 (CTG-46.95) exhibits significant up-regulation as a principal target, suppressing cell differentiation (Nguyen et al., 2025; Xiong et al., 2025), accelerating transforming growth factor- $\beta$ 1 (TGF- $\beta$ 1) transcription (Liu et al., 2024a), and ECM deposition (Vadon-Le Goff et al., 2015; Karakaya et al., 2022). In addition, the THBS family of ECM receptor interaction pathway is also jointly implicated in this process. On the one hand, the up-regulated THBS-1 can also activate TGF- $\beta$ , and TGF- $\beta$  exerts a potent effect in down-regulating the expression of metzincins and inhibiting ECM degradation as well as promoting ECM deposition (Porphiglia et al., 2022; Yan et al., 2025). On the other hand, the increased expression of THBS-2 can positively regulate the Notch pathway

(Chang et al., 2024). Therefore, we speculate that EDTA can activate the Notch pathway by chelating  $\text{Ca}^{2+}$  and up-regulating ADAM-10. The THBS family in the ECM receptor interaction pathway acts synergistically with the Notch pathway to downregulate the expression of metzincins, inhibit ECM disassembly and remodelling promote ECM deposition, resulting in the negative regulation of the budding of *A. coerulea* polyps.

Through the integrated omics analysis carried out in this study, the composition of metzincins in the polyp of *A. coerulea* was clarified, and it was confirmed that NAS was the predominant metzincins in the polyp of *A. coerulea*. Regrettably, due to restrictive conditions, this study was unable to experimentally verify the independent role of NAS in ECM degradation and the budding of *A. coerulea* polyps, which will be our future task. In this study, EDTA had an impact on the polyp of jellyfish *A. coerulea*, resulting in the reduction of metzincin activity and expression, thereby further influencing ECM remodeling and inhibiting the budding of *A. coerulea* polyps. This enabled us to identify potential targets for regulating the number of jellyfish. Subsequently, how to transform this discovery into applicable products and how to avoid the side effects of the application of EDTA in the prevention and control of jellyfish blooms on the marine ecology will be our subsequent research goals.

## 5 Conclusion

This study emphasizes that NAS metzincins are important biotoxins of *A. coerulea* polyps and are involved in regulating the budding reproduction of the polyps. EDTA can inhibit the budding of *A. coerulea* polyps by diminishing the proteolytic activity of metzincins and down-regulating their molecular expression. The ECM-receptor interaction pathway and Notch pathways cooperatively contribute to regulating this process.

Certain limitations exist in this study. Firstly, the single source of samples and the insufficiently large sample size might potentially lead to a reduction in the universality of the outcomes. The biological sample *A. coerulea* polyps employed in this study were obtained from stable breeding within the laboratory. Ideally, representative samplings should be conducted from various jellyfish blooms waters worldwide, and reliable manipulative experiments should be carried out to validate the universality of the research findings. Secondly, the exploration of the mechanism through which EDTA regulates the metzincins in this study is not profound enough. In the EDTA intervention budding experiment of polyps, altering and detecting the concentration of divalent ions in the culture environment within the experimental unit, in combination with the detection of the activity of metzincins, will contribute to further clarifying the mechanism through which EDTA regulates the activity of metzincins to inhibit the budding of polyps.

The findings have provided valuable insights into the role of biotoxins in the development and proliferation of jellyfish, and also

provided new means and a theoretical basis for the prevention and control of the jellyfish blooms.

## Data availability statement

The original contributions presented in the study are included in the article/[Supplementary Material](#). Further inquiries can be directed to the corresponding authors.

## Author contributions

XL: Data curation, Writing – original draft. XP: Data curation, Writing – original draft. SJ: Writing – review & editing, Formal Analysis. JW: Data curation, Writing – review & editing. QS: Writing – review & editing, Formal Analysis. WJ: Writing – review & editing, Resources. XH: Writing – review & editing, Formal Analysis. HZ: Writing – review & editing, Methodology. JH: Writing – review & editing, Data curation. MP: Writing – review & editing, Methodology. SX: Writing – review & editing. XM: Writing – review & editing, Formal Analysis, Methodology. LX: Writing – review & editing, Funding acquisition, Supervision.

## Funding

The author(s) declare that financial support was received for the research and/or publication of this article. This research was supported by the second phase of the 'Voyage Plan' funded by the Faculty of Naval Medicine, Naval Medical University (Second Military Medical University).

## Acknowledgments

The authors express their gratitude to Jinchi Yao for the assistance he provided in the field of molecular structure. Sincere gratitude is expressed to Naval Medical University for supporting this research.

## Conflict of interest

The authors declare that the research was conducted in the absence of any commercial or financial relationships that could be construed as a potential conflict of interest.

The author(s) declared that they were an editorial board member of *Frontiers*, at the time of submission. This had no impact on the peer review process and the final decision.

## Generative AI statement

The author(s) declare that no Generative AI was used in the creation of this manuscript.

## Publisher's note

All claims expressed in this article are solely those of the authors and do not necessarily represent those of their affiliated organizations,

or those of the publisher, the editors and the reviewers. Any product that may be evaluated in this article, or claim that may be made by its manufacturer, is not guaranteed or endorsed by the publisher.

## Supplementary material

The Supplementary Material for this article can be found online at: <https://www.frontiersin.org/articles/10.3389/fmars.2025.1563258/full#supplementary-material>.

## References

- Apte, S. S., and Parks, W. C. (2015). Metalloproteinases: A parade of functions in matrix biology and an outlook for the future. *Matrix Biol.* 44–46, 1–6. doi: 10.1016/j.matbio.2015.04.005
- Aufschnaiter, R., Zamir, E. A., Little, C. D., Özbek, S., Münder, S., David, C. N., et al. (2011). *In vivo* imaging of basement membrane movement: ECM patterning shapes Hydra polyps. *J. Cell Sci.* 124, 4027–4038. doi: 10.1242/jcs.087239
- Becker-Pauly, C., Barré, O., Schilling, O., Auf dem Keller, U., Ohler, A., Broder, C., et al. (2011). Proteomic analyses reveal an acidic prime side specificity for the astacin metalloprotease family reflected by physiological substrates. *Mol. Cell Proteomics* 10, M111.009233. doi: 10.1074/mcp.M111.009233
- Bi, W. H., Jin, Y., Wang, Y. T., Li, J. X., Zhang, H. D., Jin, W., et al. (2024). Discovery and experimental verification of the spectral characteristics at different growth stages of Aurelia. *Spectrochim Acta A Mol. Biomol. Spectrosc.* 304, 123304. doi: 10.1016/j.saa.2023.123304
- Bradford, M. M. (1976). A rapid and sensitive method for the quantitation of microgram quantities of protein utilizing the principle of protein-dye binding. *Anal. Biochem.* 72, 248–254. doi: 10.1006/abio.1976.9999
- Bryant, P., Pozzati, G., and Elofsson, A. (2022). Improved prediction of protein-protein interactions using AlphaFold2. *Nat. Commun.* 13, 1265. doi: 10.1038/s41467-022-28865-w
- Cerdà-Costa, N., and Gomis-Rüth, F. X. (2014). Architecture and function of metalloprotease catalytic domains. *Protein Sci.* 23, 123–144. doi: 10.1002/pro.2400
- Chang, Z., Gao, Y., Chen, P., Gao, W., Zhao, W., Wu, D., et al. (2024). THBS2 promotes gastric cancer progression and stemness via the Notch signaling pathway. *Am. J. Cancer Res.* 14, 3433–3450. doi: 10.62347/uxwk4038
- Chen, J., Ikeda, S. I., Yang, Y., Zhang, Y., Ma, Z., Liang, Y., et al. (2024). Scleral remodeling during myopia development in mice eyes: a potential role of thrombospondin-1. *Mol. Med.* 30, 25. doi: 10.1186/s10020-024-00795-x
- Chiarelli, R., Martino, C., Scudiero, R., Terenzi, A., and Geraci, F. (2025). Remodeling of embryo architecture in response to vanadium and increased temperatures: from morphometric to molecular changes. *J. Xenobiot* 15 (1), 22. doi: 10.3390/jox15010022
- Defamie, V., Aliar, K., Sarkar, S., Vyas, F., Shetty, R., Reddy Narala, S., et al. (2024). Metalloproteinase inhibitors regulate biliary progenitor cells through sDLK1 in organoid models of liver injury. *J. Clin. Invest.* 135 (3), e164997. doi: 10.1172/jci164997
- Dong, Z., and Sun, T. (2018). Combined effects of ocean acidification and temperature on planula larvae of the moon jellyfish *Aurelia coerulea*. *Mar. Environ. Res.* 139, 144–150. doi: 10.1016/j.marenvres.2018.05.015
- Dornier, E., Coumailleau, F., Ottavi, J. F., Moretti, J., Boucheix, C., Mauduit, P., et al. (2016). Correction: TspanC8 tetraspanins regulate ADAM10/Kuzbanian trafficking and promote Notch activation in flies and mammals. *J. Cell Biol.* 213, 495–496. doi: 10.1083/jcb.20120113304262016c
- Eberhardt, J., Santos-Martins, D., Tillack, A. F., and Forli, S. (2021). AutoDock vina 1.2.0: new docking methods, expanded force field, and python bindings. *J. Chem. Inf. Model.* 61, 3891–3898. doi: 10.1021/acs.jcim.1c00203
- Edelst, D., Angel, D. L., Barkan, N., Danino-Gozlan, C., Palanker, A., Barak, L., et al. (2023). Jellyfish sting web survey: clinical characteristics and management of *Rhopilema nomadica* envenomation in the Mediterranean Sea. *Regional Environ. Change* 23. doi: 10.1007/s10113-023-02104-4
- Fuchs, B., Wang, W., Graspeuntner, S., Li, Y., Insua, S., Herbst, E. M., et al. (2014). Regulation of polyp-to-jellyfish transition in *Aurelia aurita*. *Curr. Biol.* 24, 263–273. doi: 10.1016/j.cub.2013.12.003
- Gao, M., Li, S., Wang, K., Bai, Y., Ding, Y., Zhang, B., et al. (2023). Real-time jellyfish classification and detection algorithm based on improved YOLOv4-tiny and improved underwater image enhancement algorithm. *Sci. Rep.* 13, 12989. doi: 10.1038/s41598-023-39851-7
- García-López, C., Rodríguez-Calvo-de-Mora, M., Borroni, D., Sánchez-González, J. M., Romano, V., and Rocha-de-Lossada, C. (2023). The role of matrix metalloproteinases in infectious corneal ulcers. *Surv. Ophthalmol.* 68, 929–939. doi: 10.1016/j.survophthal.2023.06.007
- Gold, D. A., Katsuki, T., Li, Y., Yan, X., Regulski, M., Ibberson, D., et al. (2019). The genome of the jellyfish *Aurelia* and the evolution of animal complexity. *Nat. Ecol. Evol.* 3, 96–104. doi: 10.1038/s41559-018-0719-8
- Gomis-Ruth, F. X., Trillo-Muyo, S., and Stocker, W. (2012). Functional and structural insights into astacin metalloproteases. *Biol. Chem.* 393, 1027–1041. doi: 10.1515/hsz-2012-0149
- Hubot, N., Lucas, C. H., and Piraino, S. (2017). Environmental control of asexual reproduction and somatic growth of *Aurelia* spp. (Cnidaria, Scyphozoa) polyps from the Adriatic Sea. *PLoS One* 12, e0178482. doi: 10.1371/journal.pone.0178482
- Kan, T., Gui, L., Shi, W., Huang, Y., Li, S., and Qiu, C. (2016). A survey of jellyfish stinging knowledge among naval personnel in northeast China. *Int. J. Environ. Res. Public Health* 13 (7), 725. doi: 10.3390/ijerph13070725
- Karakaya, C., van Turnhout, M. C., Visser, V. L., Ristori, T., Bouten, C. V. C., Sahlgren, C. M., et al. (2022). Notch signaling regulates strain-mediated phenotypic switching of vascular smooth muscle cells. *Front. Cell Dev. Biol.* 10. doi: 10.3389/fcell.2022.910503
- Keow, J. Y., Herrmann, K. M., and Crawford, B. D. (2011). Differential *in vivo* zymography: a method for observing matrix metalloproteinase activity in the zebrafish embryo. *Matrix Biol.* 30, 169–177. doi: 10.1016/j.matbio.2011.01.003
- Khalturin, K., Shinzato, C., Khalturina, M., Hamada, M., Fujie, M., Koyanagi, R., et al. (2019). Medusozoan genomes inform the evolution of the jellyfish body plan. *Nat. Ecol. Evol.* 3, 811–822. doi: 10.1038/s41559-019-0853-y
- Kim, H. M., Weber, J. A., Lee, N., Park, S. G., Cho, Y. S., Bhak, Y., et al. (2019). The genome of the giant Nomura's jellyfish sheds light on the early evolution of active predation. *BMC Biol.* 17, 28. doi: 10.1186/s12915-019-0643-7
- Klompfen, A. M. L., Kayal, E., Collins, A. G., and Cartwright, P. (2021). Phylogenetic and selection analysis of an expanded family of putatively pore-forming jellyfish toxins (Cnidaria: medusozoa). *Genome Biol. Evol.* 13 (6), evab081. doi: 10.1093/gbe/evab081
- Kovall, R. A., Gebelein, B., Sprinzak, D., and Kopan, R. (2017). The canonical notch signaling pathway: structural and biochemical insights into shape, sugar, and force. *Dev. Cell* 41, 228–241. doi: 10.1016/j.devcel.2017.04.001
- Law, Y. H. (2018). Stopping the sting. *Science* 362, 631–635. doi: 10.1126/science.362.6415.631
- Levy, T., Ghermandi, A., Lehahn, Y., Edelst, D., and Angel, D. L. (2024). Monitoring jellyfish outbreaks along Israel's Mediterranean coast using digital footprints. *Sci. Total Environ.* 922, 171275. doi: 10.1016/j.scitotenv.2024.171275
- Li, A., Yu, H., Li, R., Liu, S., Xing, R., and Li, P. (2019). Inhibitory effect of metalloproteinase inhibitors on skin cell inflammation induced by jellyfish nemopilema nomurai nematocyst venom. *Toxins (Basel)* 11 (3), 156. doi: 10.3390/toxins11030156
- Li, A., Yu, H., Li, R., Yue, Y., Yu, C., Liu, S., et al. (2024a). Effects of toxin metalloproteinases from jellyfish *Nemopilema nomurai* nematocyst on the dermal toxicity and potential treatment of jellyfish dermatitis. *Int. Immunopharmacol.* 128, 111492. doi: 10.1016/j.intimp.2024.111492
- Li, X., Ma, X., Chen, X., Wang, T., Liu, Q., Wang, Y., et al. (2022). The medusa of *Aurelia coerulea* is similar to its polyp in molecular composition and different from the medusa of *Stomolophus meleagris* in toxicity. *Toxicol.* 210, 89–99. doi: 10.1016/j.toxicol.2022.02.006
- Li, Y., Chen, Y., Wu, W., Li, N., and Hua, J. (2023). MMPs, ADAMs and ADAMTSs are associated with mammalian sperm fate. *Theriogenology* 200, 147–154. doi: 10.1016/j.theriogenology.2023.02.013
- Li, Y., Peng, S., Liu, Y., Sun, K., Wu, L., Yu, Z., et al. (2024b). Molecular and cellular basis of life cycle transition provides new insights into ecological adaptation in jellyfish. *Innovation Geosci.* 2 (2), 100063. doi: 10.59717/j.xinn-geo.2024.100063

- Liu, W., Ding, Y., Shen, Z., Xu, C., Yi, W., Wang, D., et al. (2024b). BF170 hydrochloride enhances the emergence of hematopoietic stem and progenitor cells. *Development* 151 (13), dev202476. doi: 10.1242/dev.202476
- Liu, Q. X., Zhu, Y., Yi, H. M., Shen, Y. G., Wang, L., Cheng, S., et al. (2024a). KMT2D mutations promoted tumor progression in diffuse large B-cell lymphoma through altering tumor-induced regulatory T cell trafficking via FBXW7-NOTCH-MYC/TGF- $\beta$ 1 axis. *Int. J. Biol. Sci.* 20, 3972–3985. doi: 10.7150/ijbs.93349
- Livmore, C., Warr, N., Chalon, N., Siggers, P., Mianne, J., Codner, G., et al. (2019). Male mice lacking ADAMTS-16 are fertile but exhibit testes of reduced weight. *Sci. Rep.* 9, 17195. doi: 10.1038/s41598-019-53900-0
- Marchelek-Mysliwicz, M., Kosik-Bogacka, D., Ciechanowski, K., Marchelek, E., Lanocha-Arendarczyk, N., Grubman-Nowak, M., et al. (2024). Nephrotoxic effects of Cnidaria toxins. *Int. Marit Health* 75, 245–253. doi: 10.5603/imh.102878
- Marino, G., and Funk, C. (2012). Matrix metalloproteinases in plants: a brief overview. *Physiol. Plant* 145, 196–202. doi: 10.1111/j.1399-3054.2011.01544.x
- Marques, R., Darnaude, A. M., Schiariti, A., Tremblay, Y., Molinero, J.-C., Soriano, S., et al. (2019). Dynamics and asexual reproduction of the jellyfish *Aurelia coerulea* benthic life stage in the Thau lagoon (northwestern Mediterranean). *Mar. Biol.* 166, 74. doi: 10.1007/s00227-019-3522-4
- Mathew, S., Fu, L., Hasebe, T., Ishizuya-Oka, A., and Shi, Y. B. (2010). Tissue-dependent induction of apoptosis by matrix metalloproteinase stromelysin-3 during amphibian metamorphosis. *Birth Defects Res. C Embryo Today* 90, 55–66. doi: 10.1002/bdrc.20170
- Matsubayashi, Y. (2022). Dynamic movement and turnover of extracellular matrices during tissue development and maintenance. *Fly (Austin)* 16, 248–274. doi: 10.1080/19336934.2022.2076539
- Miao, T., Wan, Z., Sun, L., Li, X., Xing, L., Bai, Y., et al. (2017). Extracellular matrix remodeling and matrix metalloproteinases (ajMMP-2 like and ajMMP-16 like) characterization during intestine regeneration of sea cucumber *Apostichopus japonicus*. *Comp. Biochem. Physiol. B Biochem. Mol. Biol.* 212, 12–23. doi: 10.1016/j.cbpb.2017.06.011
- Morgulis, M., Winter, M. R., Shternhell, L., Gildor, T., and Ben-Tabou de-Leon, S. (2021). VEGF signaling activates the matrix metalloproteinases, MmpL7 and MmpL5 at the sites of active skeletal growth and MmpL7 regulates skeletal elongation. *Dev. Biol.* 473, 80–89. doi: 10.1016/j.ydbio.2021.01.013
- Mubarak, A. I., Wan Mohd Shukri, W. N. A., and Ismail, A. K. (2021). Estimation of local incidence of jellyfish envenomation in developed marine coastal areas and large populated island on the western coast of Peninsular Malaysia using case surveillance of government health facilities in Manjung, Perak and Langkawi Island. *Int. Marit Health* 72, 93–98. doi: 10.5603/IMH.2021.0017
- Nguyen, N. T. B., Gevers, S., Kok, R. N. U., Burgering, L. M., Neikes, H., Akkerman, N., et al. (2025). Lactate controls cancer stemness and plasticity through epigenetic regulation. *Cell Metab.* S1550-4131(25)00002-6. doi: 10.1016/j.cmet.2025.01.002
- Ohdera, A. H., Mansbridge, M., Wang, M., Naydenkov, P., Kamel, B., and Goentoro, L. (2024). The microbiome of a Pacific moon jellyfish *Aurelia coerulea*. *PLoS One* 19, e0298002. doi: 10.1371/journal.pone.0298002
- Peng, X., Dai, Z., and Wang, X. (2020). Comparative proteomic analysis to probe into the differences in protein expression profiles and toxicity bases of *Latrodectus tredecimguttatus* spiderlings and adult spiders. *Comp. Biochem. Physiol. Part C: Toxicol. Pharmacol.* 232, 108762. doi: 10.1016/j.cbpc.2020.108762
- Peters, F., and Becker-Pauly, C. (2019). Role of meprin metalloproteases in metastasis and tumor microenvironment. *Cancer Metastasis Rev.* 38, 347–356. doi: 10.1007/s10555-019-09805-5
- Porpiglia, E., Mai, T., Kraft, P., Holbrook, C. A., de Morree, A., Gonzalez, V. D., et al. (2022). Elevated CD47 is a hallmark of dysfunctional aged muscle stem cells that can be targeted to augment regeneration. *Cell Stem Cell* 29, 1653–1668.e1658. doi: 10.1016/j.stem.2022.10.009
- Rivera, S., Khrestchatsky, M., Kaczmarek, L., Rosenberg, G. A., and Jaworski, D. M. (2010). Zincin proteases and their inhibitors: foes or friends in nervous system physiology? *J. Neurosci.* 30, 15337–15357. doi: 10.1523/jneurosci.3467-10.2010
- Rose, K. W. J., Taye, N., Karoulis, S. Z., and Hubmacher, D. (2021). Regulation of ADAMTS proteases. *Front. Mol. Biosci.* 8. doi: 10.3389/fmolb.2021.701959
- Rowe, C. E., Figueira, W. F., Kelaher, B. P., Giles, A., Mamo, L. T., Ah Yong, S. T., et al. (2022). Evaluating the effectiveness of drones for quantifying invasive upside-down jellyfish (*Cassiopea* sp.) in Lake Macquarie, Australia. *PLoS One* 17, e0262721. doi: 10.1371/journal.pone.0262721
- Sarras, M. P. Jr., Yan, L., Leontovich, A., and Zhang, J. S. (2002). Structure, expression, and developmental function of early divergent forms of metalloproteinases in hydra. *Cell Res.* 12, 163–176. doi: 10.1038/sj.cr.7290123
- Shimizu, H., Hosseini-Alghaderi, S., Woodcock, S. A., and Baron, M. (2024). Alternative mechanisms of Notch activation by partitioning into distinct endosomal domains. *J. Cell Biol.* 223 (5), e202211041. doi: 10.1083/jcb.202211041
- Song, Y., Wang, T., Xiong, M., Yang, S., Zhang, H., Ying, J., et al. (2024). Analysis of the distribution characteristics of jellyfish and environmental factors in the seawater intake area of the haiyang nuclear power plant in China. *Biol. (Basel)* 13 (6), 433. doi: 10.3390/biology13060433
- Stabili, L., Rizzo, L., Caprioli, R., Leone, A., and Piraino, S. (2021). Jellyfish bioprospecting in the mediterranean sea: antioxidant and lysozyme-like activities from *aurelia coerulea* (Cnidaria, scyphozoa) extracts. *Mar. Drugs* 19 (11), 619. doi: 10.3390/md19110619
- Sterchi, E. E., Stöcker, W., and Bond, J. S. (2008). Meprins, membrane-bound and secreted astacin metalloproteinases. *Mol. Aspects Med.* 29, 309–328. doi: 10.1016/j.mam.2008.08.002
- Vadon-Le Goff, S., Hulmes, D. J., and Moali, C. (2015). BMP-1/tolloid-like proteinases synchronize matrix assembly with growth factor activation to promote morphogenesis and tissue remodeling. *Matrix Biol.* 44–46, 14–23. doi: 10.1016/j.matbio.2015.02.006
- Wang, J., Ma, X., Gao, X., Liu, Q., Wang, Y., Xia, W., et al. (2023). Glutathione metabolism is conserved in response to excessive copper exposure between mice liver and *Aurelia coerulea* polyps. *Sci. Total Environ.* 881, 163382. doi: 10.1016/j.scitotenv.2023.163382
- Weiland-Brauer, N., Pinnow, N., Langfeldt, D., Roik, A., Gullert, S., Chibani, C. M., et al. (2020). The native microbiome is crucial for offspring generation and fitness of *aurelia aurita*. *mBio* 11 (6), e02336-20. doi: 10.1128/mBio.02336-20
- Xiong, Y., Weng, Y., Zhu, S., Qin, J., Feng, J., Jing, X., et al. (2025). NOX4 modulates breast cancer progression through cancer cell metabolic reprogramming and CD8(+) T cell antitumor activity. *Front. Immunol.* 16. doi: 10.3389/fimmu.2025.1534936
- Yan, X., Ding, J. Y., Zhang, R. J., Wang, Y. X., Zhou, L. P., Zhang, H. Q., et al. (2025). FSTL1 accelerates nucleus pulposus-derived mesenchymal stem cell apoptosis in intervertebral disc degeneration by activating TGF- $\beta$ -mediated Smad2/3 phosphorylation. *J. Transl. Med.* 23, 232. doi: 10.1186/s12967-025-06231-w
- Yanagihara, A. A., Giglio, M. L., Hurwitz, K., Kadler, R., Espino, S. S., Raghuraman, S., et al. (2024). Elucidation of medusozoan (Jellyfish) venom constituent activities using constellation pharmacology. *Toxins (Basel)* 16 (10), 447. doi: 10.3390/toxins16100447
- Yasanga, T., Wunnapuk, K., Phuackchantuck, R., Thaikrua, L., Achalawitkun, T., Rungraung, P., et al. (2025). Updated Nematocyst Types in Tentacle of Venomous Box Jellyfish, *Chironex indrasaksajiae* (Sucharitakul 2017) and *Chirospoides buitendijki* ((Horst 1907)) (Cnidaria, Cubozoa) in Thai Waters. *Toxins (Basel)* 17 (1), 44. doi: 10.3390/toxins17010044